Available online at www.sciencedirect.com

ScienceDirect

Nuclear Data Sheets 119 (2014) 310–313

Nuclear Data Sheets

www.elsevier.com/locate/nds

Partial Photoneutron Cross Sections for ^{207,208}Pb

T. Kondo,[1] H. Utsunomiya,[1,*] S. Goriely,[2] C. Iwamoto,[1] H. Akimune,[1] T. Yamagata,[1] H. Toyokawa,[3] H. Harada,[4] F. Kitatani,[4] Y.-W. Lui,[5] S. Hilaire,[6] and A.J. Koning[7]

[1] *Department of Physics, Konan University, Okamoto 8-9-1, Higashinada, Kobe 658-8501, Japan*
[2] *Institut d'Astronomie et d'Astrophysique, Université Libre de Bruxelles, Campus de la Plaine, CP-226, 1050 Brussels, Belgium*
[3] *National Institute of Advanced Industrial Science and Technology, Tsukuba 305-8568, Japan*
[4] *Japan Atomic Energy Agency, Tokai-mura, Naka, Ibaraki 319-1195, Japan*
[5] *Cyclotron Institute, Texas A&M University, College Station, Texas 77843, USA*
[6] *CEA, DAM, DIF, F-91297 Arpajon, France*
[7] *Nuclear Research and Consultancy Group, P.O. Box 25, NL-1755 ZG Petten, The Netherlands*

Using linearly-polarized laser-Compton scattering γ-rays, partial $E1$ and $M1$ photoneutron cross sections along with total cross sections were determined for ^{207,208}Pb at four energies near neutron threshold by measuring anisotropies in photoneutron emission. Separately, total photoneutron cross sections were measured for ^{207,208}Pb with a high-efficiency 4π neutron detector. The partial cross section measurement provides direct evidence for the presence of pygmy dipole resonance (PDR) in ^{207,208}Pb in the vicinity of neutron threshold. The strength of PDR amounts to 0.32% - 0.42% of the Thomas-Reiche-Kuhn sum rule. Several μ_N^2 units of $B(M1)\uparrow$ strength were observed in ^{207,208}Pb just above neutron threshold, which correspond to M1 cross sections less than 10% of the total photoneutron cross sections.

I. INTRODUCTION

The γ-ray strength function (γSF) below neutron threshold, along with the nuclear level density, is a key physics quantity of the Hauser-Feshbach model calculations of radiative neutron capture cross sections in the field of nuclear astrophysics and nuclear engineering. Recently pygmy dipole resonance (PDR) and M1 resonance have drawn much attention because they constitute extra strengths of γSF. The nuclear resonance fluorescence technique (NRF) using linearly -polarized γ rays is used to separate $E1$ and $M1$ strengths for resolved peaks below neutron threshold by identifying ground-state transitions [1]. The technique is also used for quasi-continuum components though the strength determination is not so straightforward. The NRF technique is well suited to investigate even-even nuclei with high neutron threshold. The 0^+ ground state in even-even nuclei simplifies the identification of ground-state transitions in the NRF technique.

Photoneutron cross sections directly provide γSF above neutron threshold, thus constraining the gross structure of the γSF in the low-energy tail of the giant dipole resonance. Furthermore, one can detect, through photoneutron cross section measurements, PDR for odd-N nuclei with neutron thresholds as low as 6 - 7 MeV. We have measured photoneutron cross sections with a 4π neutron detector to investigate the γSF including PDR [2]. In this paper, we report results of a new experimental attempt to separate E1 and M1 strengths in ^{207,208}Pb by measuring anisotropies in photoneutron emission.

II. ANISOTROPY MEASUREMENT

The experimental principle of separating $E1$ and $M1$ strengths is depicted in Fig. 1. In the $E1$ and $M1$ photoexcitations of ^{208}Pb, 1^- and 1^+ states are, respectively, populated and decay to the ground state $1/2^-$ in ^{207}Pb by s-wave and p-wave neutron emissions. It is to be noted that in the energetically-allowed decay to low-lying excited states in ^{207}Pb, the s-wave and p-wave emission are accompanied by d-wave and f-wave emissions, respectively. However, when the excitation energy is not too high, the d-wave and f-wave emissions are, in general, suppressed by the centrifugal potential. A similar discussion is applied to photoexcitation of ^{207}Pb except that the E1 photoexcitation populates both $1/2^+$ and $3/2^+$ states, the latter of which can decay to the ground state 0^+ in ^{206}Pb by d-wave neutron emission. The s-wave neutrons are emitted isotropically, while the p-wave neutrons are emitted preferentially along the linear polar-

* Corresponding author: hiro@konan-u.ac.jp

http://dx.doi.org/10.1016/j.nds.2014.08.085

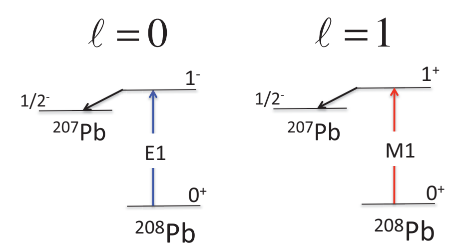

FIG. 1. $E1$ and $M1$ photoexcitations of ^{208}Pb leading to s-wave and p-wave neutron emissions.

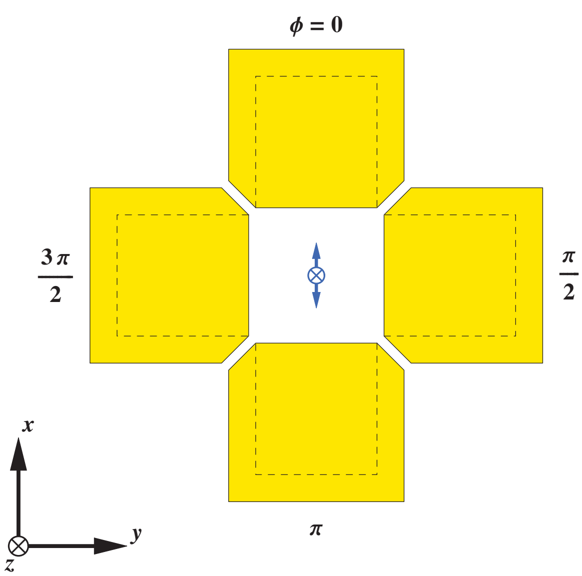

FIG. 2. Experimental setup of four sets of neutron detectors for a vertically polarized γ-ray beam.

ization. Therefore, it is possible to separate E1 and M1 photoexcitations by measuring anisotropy of photoneutron emission.

The experiment was performed at the National Institute for Advanced Industrial Science and Technology. Enriched ^{207}Pb (99.1% 3482 mg) and ^{208}Pb (98.5% 9587 mg) metal samples shaped in 8mm diameter were irradiated by linearly-polarized laser Compton scattering γ-ray beams at four energies near the neutron threshold, respectively. The linear polarization was 93.4 ± 0.7% after a slight depolarization caused by the laser optics (two lenses and one mirror). The neutron detection system is shown in Fig. 2. Four units of high- and flat-efficiency long counters of East and Walton type [3] with five ^{3}He proportional counters embedded in a polyethylene moderator and twelve neutron-guiding holes were mounted at the distance 125mm from the target: two at the vertical positions and two at the horizontal positions. The whole system was rotated by 90° around the beam axis and the polarization was flipped by 90° with a $\lambda/2$ optical element to reduce the systematic uncertainty associated with a possible asymmetry in the geometrical configuration of the four long counters.

The data reduction was carried out, neglecting multipoles higher than E1 and M1 photoexcitations and orbital angular momenta higher than s-wave and p-wave. The angular distributions for the s-wave emission W^s, p-wave emission induced by linearly-polarized photons W^p_{pol}, and p-wave emission induced by depolarized photons W^p_{dep} are, respectively, expressed as

$$W^s(\theta, \phi) = \frac{1}{4\pi}, \tag{1}$$

$$W^p_{pol}(\theta, \phi) = \frac{3}{8\pi}[\sin^2\theta(1 + \cos 2\phi)], \tag{2}$$

and

$$W^p_{dep}(\theta, \phi) = \frac{3}{8\pi}\sin^2\theta. \tag{3}$$

It is noted that the depolarization occurs in a plane perpendicular to the γ-ray beam axis. Here θ stands for the polar angle for photoneutron emission with respect to the beam direction (z-axis), while ϕ for the azimuthal angle with respect to the x-axis.

There are four kinds of neutron detection efficiencies: one for s-wave neutron emission ε^0, two for p-wave neutron emission induced by linearly-polarized photons $\varepsilon^1_{\parallel}$ and $\varepsilon^1_{\perp}$, and one for p-wave neutron emission induced by depolarized photons ε^1. The four counters have the same efficiencies in ε^0 and ε^1. The two counters mounted parallel to the linear polarization have $\varepsilon^1_{\parallel}$, while the two mounted perpendicular to the polarization have $\varepsilon^1_{\perp}$. The four intrinsic efficiencies are shown in Fig. 3. The ε^0 was measured with a calibrated ^{252}Cf source. The measurement agrees with the MCNP Monte Carlo simulation within 6%. The other three efficiencies were obtained by the Monte Carlo simulations.

The total and partial ($E1$ and $M1$) cross sections (σ_{tot}, σ_{E1}, and σ_{M1}) are given by

$$\sigma_{tot} = \frac{N_{tot}}{N_t N_\gamma}, \tag{4}$$

$$\sigma_{E1} = R^0\sigma_{tot}, \tag{5}$$

and

$$\sigma_{M1} = R^1\sigma_{tot}, \tag{6}$$

where N_γ is the number of incident γ rays, N_t is the areal density of the target nuclei, N_{tot} is the total number of neutrons emitted, and R^0 and R^1 are the probabilities of emitting s-wave and p-wave neutrons, respectively. Under the present assumption, R^0+R^1=1. The N_{tot}, R^0 and R^1 are determined by experimental quantities such as the polarization, the four neutron detection efficiencies, neutron yields of the four long counters, and the analyzing power of the neutron detection system. The analyzing power which is defined by

$$A = \frac{\varepsilon^1_{\parallel}(pol) - \varepsilon^1_{\perp}(pol)}{2\varepsilon^1}, \tag{7}$$

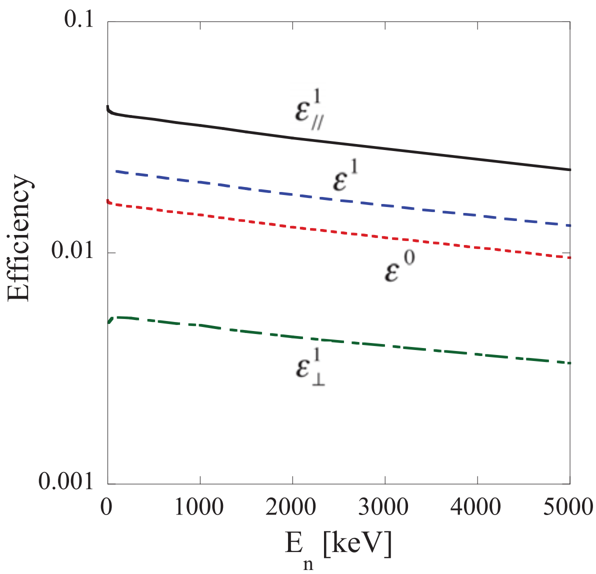

FIG. 3. Detection efficiencies for p-wave neutrons for a long counter mounted parallel to the polarization (solid line, $\varepsilon^1_{\parallel}$), perpendicular to the polarization (dot-dashed line, $\varepsilon^1_{\perp}$), for p-wave neutrons induced by depolarized photons (dashed line, ε^1), and for s-wave neutrons (dotted line, ε^0).

is 0.81 - 0.75 in the neutron energy range 1 - 5000 keV. The formulae for N_{tot}, R^0 and R^1 are found in the literature [4].

III. RESULTS AND DISCUSSIONS

Electric dipole ($E1$) cross sections for ^{208}Pb and ^{207}Pb are shown in Fig. 4. The present measurement provides direct evidence for the presence of extra strengths that can be attributed to PDR in the vicinity of neutron threshold, where PDR is partially observed in ^{208}Pb with a neutron threshold at 7.37 MeV and fully observed in ^{207}Pb with a threshold at 6.74 MeV. Total photoneutron cross sections for ^{207}Pb are also shown in Fig. 5. We remark that while the PDR is observed in ^{208}Pb in both (γ,γ') [7–11] and (p,p') [12, 13] measurements, experimental information on PDR in ^{207}Pb is very limited [7, 10] though the (γ,n) cross section of Ref. [5] seems to show an enhancement near threshold that is consistent with the present result.

To highlight the presence of PDR, the Hartree-Fock-Bogoliubov plus quasiparticle random phase approximation (HFB+QRPA) calculation [14] supplemented with a PDR is shown to be in good agreement with the data. Here the PDR is parametrized by a centroid energy 7.5 MeV, a width 0.4 MeV and a peak cross section 15 mb for ^{207}Pb (20 mb for ^{208}Pb) in Lorentzian shape. The PDR dominates the total strength near neutron threshold though the strength remains small in the unit of the Thomas-Reiche-Kuhn (TRK) sum rule: 0.42% for ^{208}Pb and 0.32% for ^{207}Pb. The reduced $E1$ transition probability $B(E1)\uparrow$ corresponding to the partial $E1$ cross section is 0.82 ± 0.09 e^{2}fm^2 over the E = 7.51 - 8.32 MeV for ^{208}Pb and 0.88 ± 0.17 e^{2}fm^2 over the E = 7.02 - 8.32 MeV for ^{207}Pb. The high-resolution inelastic proton scattering [12] found $E1$ strength in ^{208}Pb above neutron threshold, $B(E1)\uparrow$ = 0.982 ± 0.206 e^{2}fm^2 over the E = 7.515 - 8.430 MeV. The present $E1$ strength agrees well with the result of the (p,p') measurement.

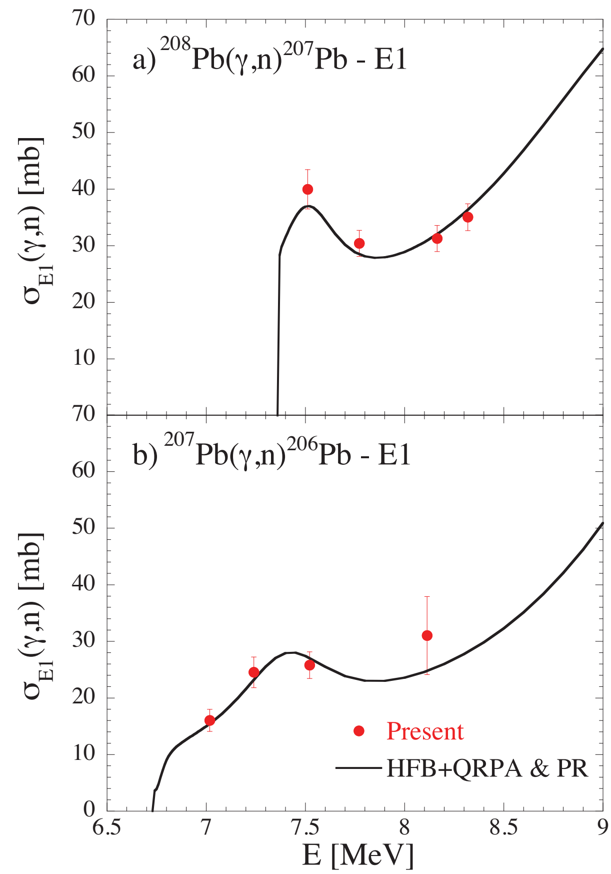

FIG. 4. (a) Comparison between experimental and theoretical ^{208}Pb(γ,n)^{207}Pb partial $E1$ cross sections. The solid line corresponds to the HFB+QRPA $E1$ strength [14] with a parametrized PDR as described in the text. (b) Same as the upper panel for the ^{207}Pb(γ,n)^{206}Pb partial $E1$ cross sections.

In contrast, magnetic dipole ($M1$) cross sections found in the present experiment are rather small, corresponding to 5.5% and 8.2% of the total cross sections for ^{208}Pb and ^{207}Pb, respectively. The reduced $M1$ transition probability $B(M1)\uparrow$ is 4.2 ± 2.3 μ_N^2 over E = 7.51 - 8.32 MeV for ^{208}Pb and 4.0 ± 1.9 μ_N^2 over E = 7.02 - 7.52 MeV for ^{207}Pb. The neutron capture measurement for ^{208}Pb [15] found 6.8 μ_N^2 over 7.37 - 8.67 MeV for resolved peaks

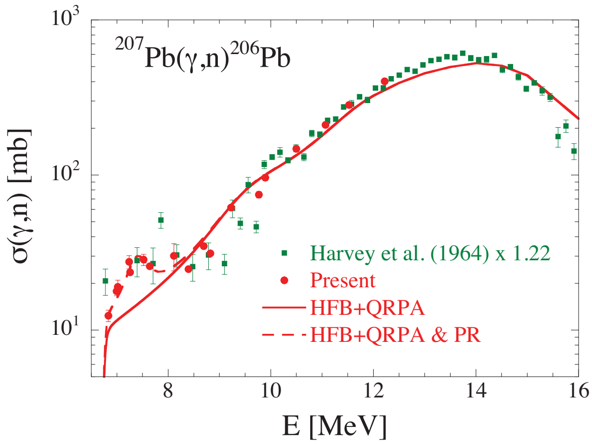

FIG. 5. Comparison between experimental and theoretical ^{207}Pb(γ,n)^{206}Pb total cross sections. Prediction as obtained with HFB+QRPA $E1$ strength with a parameterized PDR as described in the text. The experimental data are taken from [5] in addition to the present data. Note that following Ref. [6], the Livermore data are renormalized up by 22%.

with 1^+ assignment. We remark that although the $M1$ strengths of the two measurements reasonably agree with each other, the profile of the strength distribution is quite different.

IV. CONCLUSIONS

We have shown the experimental feasibility of determining $E1$ and $M1$ cross sections in photoneutron channel by measuring anisotropies in photoneutron emission under the condition that the multipoles higher than electric and magnetic dipoles and the orbital angular momenta higher than s- and p-waves are neglected. The anisotropy measurement enables one to single out pygmy dipole resonance especially in odd-N nuclei with low neutron thresholds. The present experiment which can determine full $E1$ and $M1$ strengths including continuum above neutron threshold is complementary to the nuclear resonance fluorescence experiment which can determine $E1$ and $M1$ strengths for resolved peaks below neutron threshold.

Acknowledgements: This work was supported by the Japan Private School Promotion Foundation and the Konan-ULB bilateral project. S.G. acknowledges the financial support of the "Actions de recherche concertées (ARC)" from the "Communauté française de Belgique" and from the F.N.R.S.

[1] N. Pietralla *et al.*, Phys. Rev. Lett. **88**, 012502 (2001).
[2] H. Utsunomiya *et al.*, , Phys. Rev. C **80**, 055806 (2009).
[3] L.V. East, R.B. Walton, Nucl. Instrum. Methods A **72**, 161 (1969).
[4] T. Kondo *et al.*, Phys. Rev. C **86**, 014316 (2012).
[5] R.R. Harvey, J.T. Caldwell, R.L. Bramblett, and S.C. Fultz, Phys. Rev. **136**, B126 (1964).
[6] Handbook on Photonuclear Data for Applications, IAEA TECDOC-1178 (2000).
[7] T. Chapuran, R. Vodhanel, M.K. Brussel, Phys. Rev. C **22**, 1420 (1980).
[8] R.M. Laszewski *et al.*, Phys. Rev. Lett. **61**, 1710 (1988).
[9] N. Ryezayeva *et al.*, Phys. Rev. Lett. **89**, 272502 (2002).
[10] J. Enders *et al.*, Nucl. Phys. A **724**, 243 (2003).
[11] R. Schwengner *et al.*, Phys. Rev. C **81**, 054315 (2010).
[12] A. Tamii *et al.*, Phys. Rev. Lett. **107**, 062502 (2011).
[13] I. Poltoratska *et al.*, Phys. Rev. C **85**, 041304(R) (2012).
[14] S. Goriely, E. Kahn, M. Samyn, Nucl. Phys. A **739**, 331 (2004).
[15] R. Köhler *et al.*, Phys. Rev. C **35**, 1646 (1987).